The Occurrence of Breathers and Wave-trains in a Triple Layer Stratified Fluid

Navdeep Brar

November 15, 2025

A report
presented to the University of Waterloo
in fulfillment of the report requirement for PHYS 437A Research Project

I hereby declare that I am the sole author of this report. This is a true copy of the report, including any required final revisions, as accepted by my examiners.
I understand that my report may be made electronically available to the public.

Abstract

This research delves into the phenomena of breathers and wave-trains within the context of internal gravity waves. The study begins with an introduction to internal gravity waves and their importance in oceanography. Subsequently, attention is directed towards the Gardner and modified Korteweg-de Vries (mKdV) equations, serving as the governing mathematical equations used to model a special type of internal wave called 'breathers'. Additionally, internal breathers and wave-trains are presented, and their distinguishing features are examined.

The occurrence of breathers and wave-trains under differing background conditions was then analyzed. Wave-trains were discovered to only occur within a limited range of widths and negative amplitudes. Breathers occurred for both negative and positive amplitudes and a wide range of widths. Furthermore, a comparative analysis between simulation phase speeds and theoretical predictions was done. Additionally, analytical breather solutions of the mKdV equation were compared with simulation-derived breathers, demonstrating the effectiveness of the mKdV breather solution in modeling breather solutions.

Contents

List of Figures

List of Tables

1 Introduction

1.1 Internal Gravity Waves

Internal gravity waves are waves that propagate within a fluid medium due to buoyancy forces resulting from variations in density. Unlike surface waves; which occur at the interface between two fluids of different densities; causing an abrupt change in the density (such as water and air), internal gravity waves propagate within a stratified fluid where density varies continuously with depth.

Internal gravity waves can interact with each other and with other fluid motions, leading to phenomena such as wave breaking, wave interference, and wave energy transfer[1]. These interactions play a crucial role in mixing processes and the redistribution of energy and momentum within the fluid. Internal gravity waves are found in various natural environments, including the ocean, the atmosphere, and the interiors of stars and planets. They play a significant role in ocean circulation, atmospheric dynamics, and the transport of heat, momentum, and nutrients in stratified fluid layers.

2 Introduction to the Gardner and mKdV Equation

The Gardner equation 1 is a nonlinear partial differential equation that describes wave propagation in certain physical systems, particularly in the context of nonlinear optics and nonlinear waves in dispersive media.

$$\overbrace{\underbrace{\frac{\partial \eta}{\partial t} + c_0 \frac{\partial \eta}{\partial x} + \alpha_1 \eta^2 \frac{\partial}{\partial \eta} + \beta \frac{\partial^3 \eta}{\partial x^3}}_{\text{mKdV equation}} + \alpha \eta \frac{\partial \eta}{\partial x}}^{\text{Gardner Equation}} = 0 \tag{1}$$

where η is the vertical isopycnal displacement, x is the horizontal coordinate, t is time, c_0 is the linear long-wave speed, α is the quadratic nonlinear coefficient, α_1 is the cubic nonlinear coefficient and β is the dispersion coefficient.

The addition of non-linear terms such as $\eta \frac{\partial \eta}{\partial x}$ and $\eta^2 \frac{\partial \eta}{\partial x}$ introduce non-linear effects. One consequence of these non-linear terms is that larger amplitude waves propagate faster. The $\frac{\partial^3 \eta}{\partial x^3}$ term introduces a phenomena called dispersion (discussed in section 2.3).

Our simulation utilizes a symmetric Boussinesq three-layer stratification with upper depth $h = 0.3$, total depth $H = 1$, reference density $\rho_0 = 1$ and density jump $\Delta\rho = 0.5$ across

both interfaces and gravity $g = 1$ (note that we have non-dimensionalized these variables). The coefficients in the Gardner equation for rightward- and leftward-propagating waves are given by [3]:

$$
\begin{aligned}
c_0 &= \sqrt{0.5gh} \approx 3.751 \cdot 10^{-1} \\
\alpha &= 0 \\
\alpha_1 &= -\frac{3c_0}{4h^2}(13 - \frac{9H}{2h}) \approx 4.597 \\
\beta &= \frac{c_0 h}{4}(H - \frac{4h}{3}) \approx 1.785 \cdot 10^{-2}
\end{aligned}
$$

Under this stratification, the Gardner equation simplifies to the mKdV equation. Under the condition $\frac{h}{H} < \frac{9}{26}$ the mKdV equation has breathers as a possible solution [3].

2.1 Internal Breathers

Breather solutions to the Modified Korteweg-de Vries (mKdV) equation 1 are special types of solitary wave solutions that exhibit periodic oscillations in both time and space [2]. These solutions are characterized by their ability to maintain a wave-envelope while internal waves inside this envelope oscillate periodically. See figure 1.

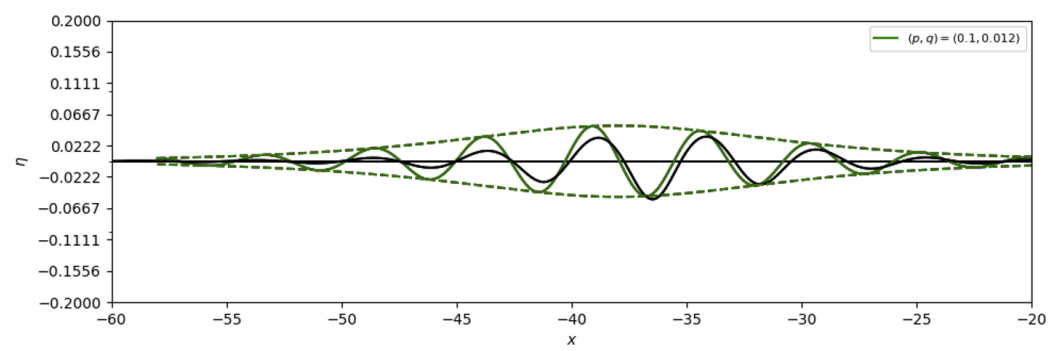

Figure 1: A breather solution (black solid lines) from the simulation overlayed by a wave envelope (green dotted line) and an analytical breather solution to the mKdV equation (green solid line). The solid black wave inside the envelope will oscillate while the wave envelope shape is fixed. The (q, p) values are parameters for the analytical breather.

Using a reference frame moving with the linear long wave speed c_0, the breather solutions to the mKdV equation have the form [3]:

$$
\eta = -\frac{4qH}{\cosh(\theta)}\left[\frac{\cos(\varphi) - (q/p)\sin(\varphi)\tanh(\theta)}{1 + (q/p)^2 \sin^2(\varphi)\,\mathrm{sech}^2(\theta)}\right] \tag{2}
$$

where q, p are parameters for the breather and φ, θ are the "carrier" and "envelope" phases respectively. We can see that for $p >> q$ we get the "envelope" of the breather (green dotted

line in figure 1) is given by:

$$\eta_{env} = -\frac{4qH}{\cosh(\theta)}$$

2.2 Wave-Trains

Wave-trains are characterized by a train of waves propagating upstream (see figure 2). These waves have a differing phase speed and group velocity due to a phenomena called dispersion which will be discussed in section 2.3.

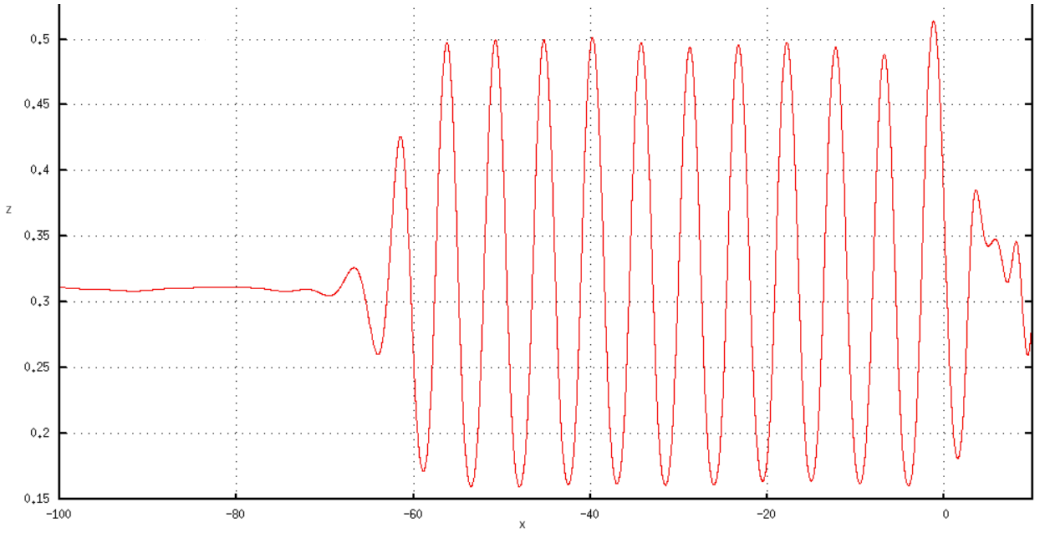

Figure 2: This figure shows a wave-train propagating upstream along a pycnocline at z=-0.3. A background current of 0.3 and a bump with amplitude -0.04 and width 0.8 were utilized.

2.3 Dispersion

Dispersion refers to the phenomenon where different spatial frequencies of a wave propagate at different speeds, causing the wave to spread out over time. This effect arises due to the dependence of wave velocity on wavelength or wave number.

2.4 Dispersion Relation for Internal Gravity Waves

Surface gravity waves exhibit a dispersion relation given by [1]

$$\omega^2 = g'k \tanh kH \tag{3}$$

Where ω is the frequency, k is the wave number, $g' = \frac{\Delta\rho}{\rho_0} g$ is the reduced gravity and H is the height of the fluid. From the dispersion relation, we can compute two quantities, the phase speed (C_s) and group velocity (C_g) [1].

The phase speed is given by:

$$C_p = \frac{\omega}{k} \tag{4}$$

This depicts the speed at which crests/troughs of the wave propagate.

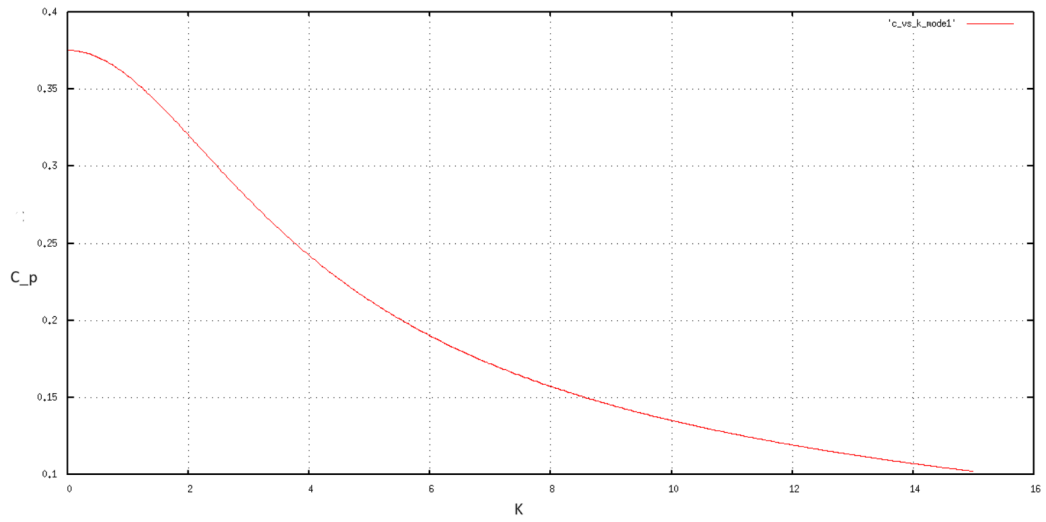

Figure 3: Phase speed vs wave number k is plotted for the parameters in section 2.0

The group velocity is given by:

$$C_g = \frac{\partial \omega}{\partial k} \tag{5}$$

This depicts the speed at which a wave envelope propagates.

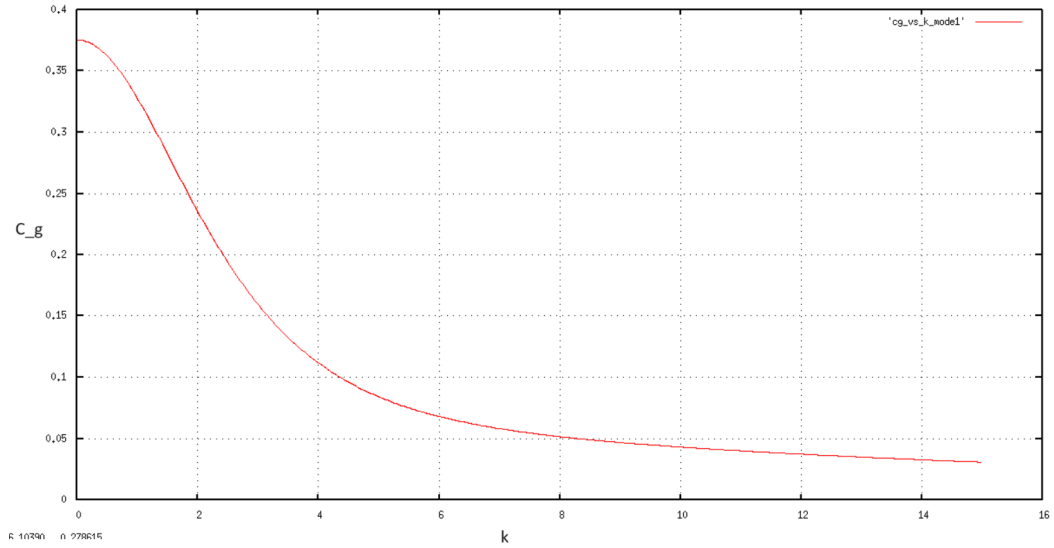

Figure 4: Group velocity vs wave number k is plotted for the parameters in section 2.0

For dispersion relations that are linear (or affine); the phase speed and group velocity

coincide. For internal gravity waves 3 we obtain that the phase speed is:

$$C_p = \sqrt{\frac{g}{k}\tanh kh}$$

an important case occurs for long waves ($kh << 1$), we then obtain that:

$$C_g = C_p = \sqrt{gh}$$

in the long wave limit we have that the phase speed and group velocity are equal and these are the fastest waves propagating up stream. As the wave number increases (wave length λ decreases) the phase speed and group velocity decrease (see figure 4 and 3).

In the opposite extreme; short waves ($kh >> 1$) we obtain:

$$C_p = \sqrt{\frac{g}{k}}$$
$$C_g = \frac{1}{2}C_p$$

we have that in the short wave limit, the group velocity is half the phase speed.

3 Experimental Techniques

In this project, a triple layer stratification was utilized; which has two distinct pycnoclines (See figure 5). One pycnocline is at $z = -0.3$ the other is at $z = -0.7$. At $x = 0$ there is a bump/hole along the seabed topography. As the background current interacts with this bump/hole; it produces disturbances in the pycnocline that generates waves.

The goal of this study was to gain a deeper understanding of the relationship between the generated wave types, background current, and bump/hole size. This was accomplished by employing a simulation that solves the inviscid Navier-Stokes equation. The back ground currents and bump amplitudes/widths were varied to find under what conditions specific waves were generated. The simulations were then compared with analytical solutions for breather in the mKdV equation. The phase speeds of wave-trains from the simulations were also compared with the theoretical phase speeds from the dispersion relation 3 (see figure 3).

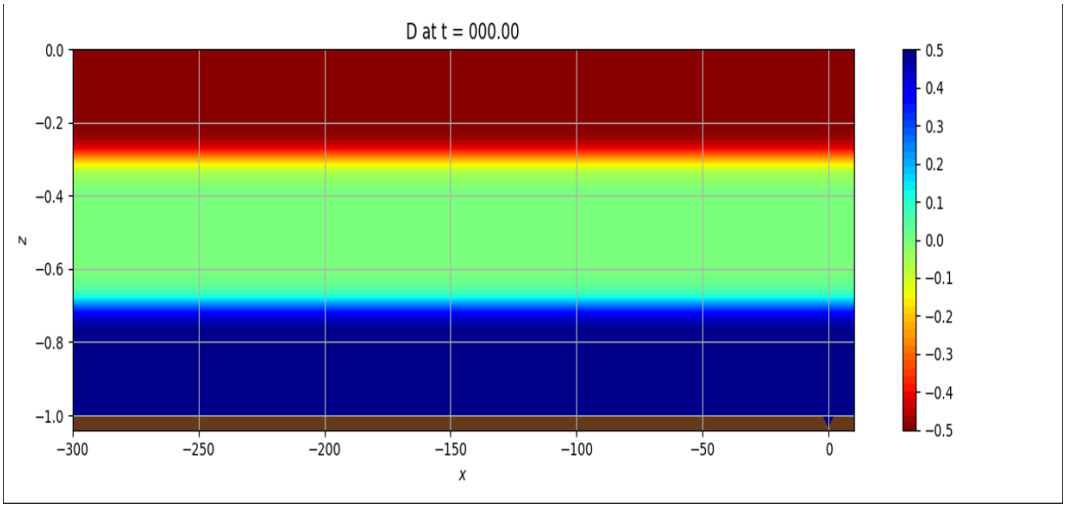

Figure 5: This figure shows a triple layer stratification. There are two distinct pycnoclines at z=-0.3 and z=-0.7 and a continuously varying density with depth throughout. The brown color at the bottom depicts the seabed topography.

4 Results

4.1 The Occurrence of Breathers and Wavetrains

For a background current of 0.29, the widths were allowed to vary between 0.5 and 2.0; the amplitudes were allowed to vary between -0.05 and 0.06 (see figure 6).

A blue triangle depicts no breather/wave-train propagating upstream. A green star depicts the occurrence of a breather propagating upstream. An orange diamond depicts a wave-train propagating upstream. A red square depicts multiple waves interacting with each other; making it impossible to discern what kind of waves are appearing.

For small amplitudes between -0.01 to 0.01 no breather or wave-train was seen to propagate upstream. Wave-trains were found to only occur for negative amplitudes (-0.04 to -0.05) and a narrow range of widths (0.9 to 1.1). Breathers were found to occur for positive amplitudes (0.025 to 0.5) and a large range of widths (0.9 to 1.4) and also negative amplitudes (-0.03 to -0.04) and widths between 0.5 and 0.9. For large widths, no breathers or wave-trains appeared.

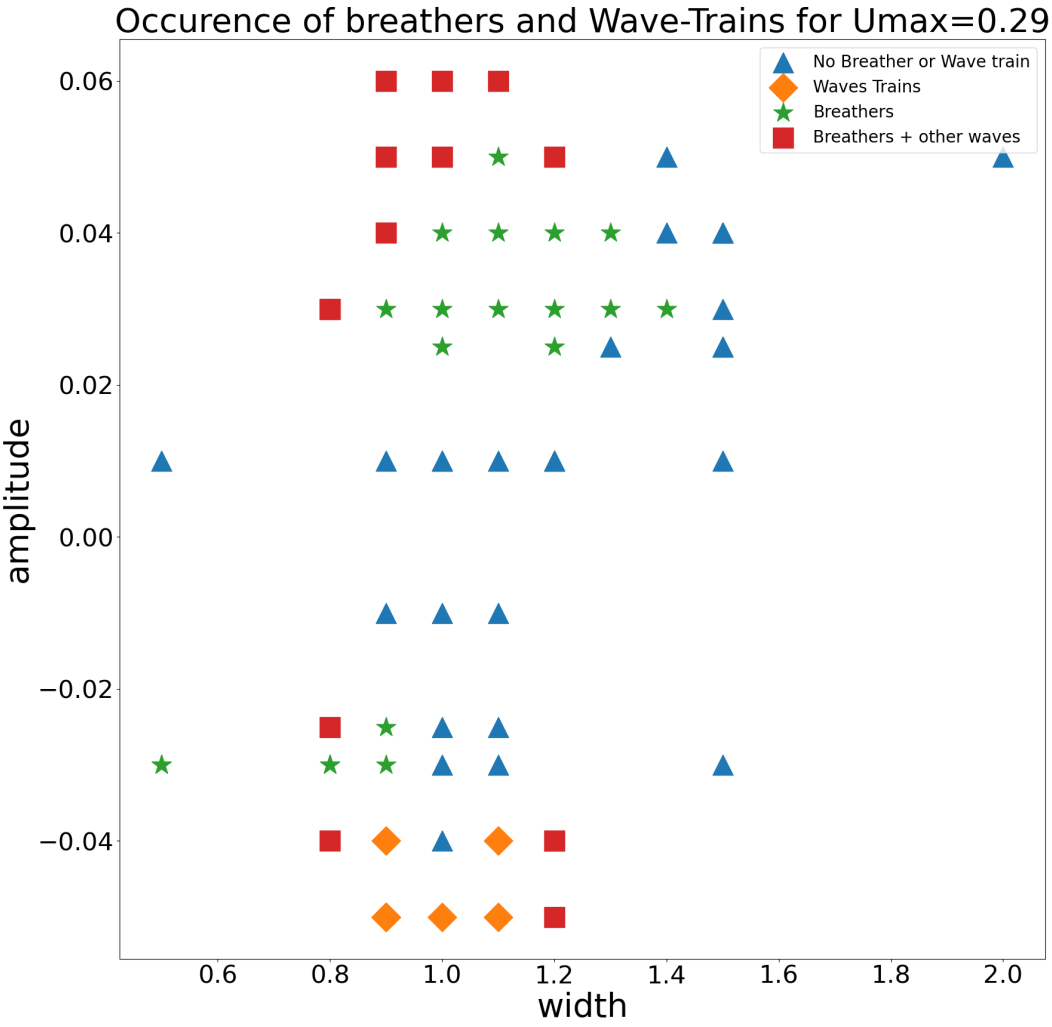

Figure 6: This plot shows the regions in parameter space (amplitude vs width) for the occurrence of breathers and wave-trains for a background current of 0.29.

For a background current of 0.3, the widths were allowed to vary between 0.5 and 2.0; the amplitudes were allowed to vary between -0.05 and 0.06 (see figure 7).

For small amplitudes between -0.01 to 0.01 no breather or wave-train was seen to propagate upstream. Wave-trains were found to only occur for negative amplitudes (-0.04 to -0.06) and a wide range of widths (0.7 to 1.2). Breathers were found to occur for positive amplitudes (0.025 to 0.5) and a large range of widths (0.5 to 1.1) and also negative amplitudes (-0.03 to -0.04) and widths between 0.5 and 0.8. For large widths, no breathers or wave-trains appeared.

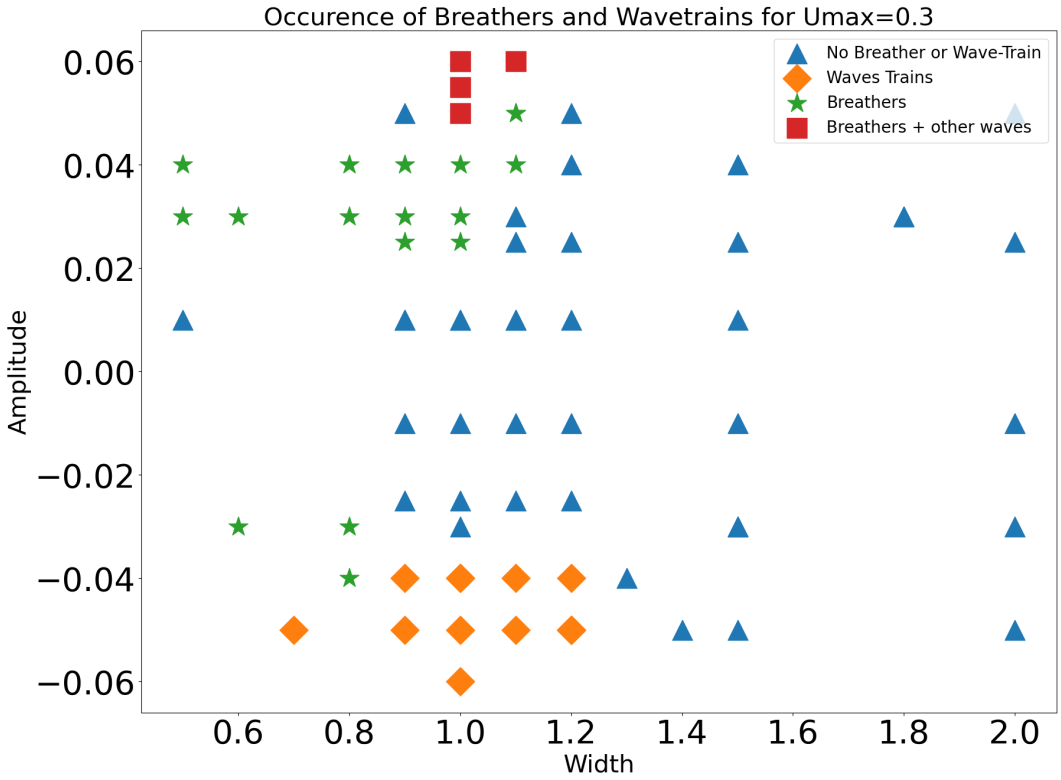

Figure 7: This plot shows the regions in parameter space (amplitude vs width) for the occurrence of breathers and wave-trains for a background current of 0.30.

For both background currents (0.3 and 0.29) we have that for large widths (greater than 1.4) no breather or wave-train was seen propagating upstream. Similarly, wave-trains were also seen to only occur for negative amplitudes; however, for a background current of 0.3, wave-trains occurred for a wider range of widths as compared to a background current of 0.29.

Breathers were seen to occur for both positive and negative amplitudes for both background currents. For positive amplitudes, breathers occurred for a wide range of widths; however, for negative amplitudes they occurred for a narrower range of widths.

4.2 Comparing Phase speeds from Simulation and Theory

The phase speed of the wave-trains from the simulation were compared with the theoretical phase speeds (see table 1). The simulation speeds were found to be in agreement with the theoretical predictions. The minor discrepancies can be explained by non-linear effects that the theoretical predictions ignore. The non-linear terms in the mKdV equation cause larger amplitude waves to propagate faster, which led to simulation phase speeds to be larger than the theoretical phase speeds.

Background Current	Amplitude	Width	Simulation C_p ± 0.0001	Theoretical C_p ± 0.0001
0.3	0.06	1	0.3581	0.3512
0.3	-0.04	1	0.3566	0.3509
0.29	-0.05	1	0.3624	0.3448
0.3	-0.05	0.7	0.3680	0.3509
0.29	-0.05	0.9	0.3454	0.3581

Table 1: Table of simulation and theoretical phase speeds for various amplitude, widths and background currents.

4.3 Comparing Analytical Breather Solutions of the mKdV equation with Simulation Breathers

The following figures are analytical breather solutions to the mKdV equation overlayed on breathers from the simulations. To determine the best fit to the simulation breathers, the (q, p) parameters of the analytical breather solution are used. Though there are minor differences, the two fit together quite well.

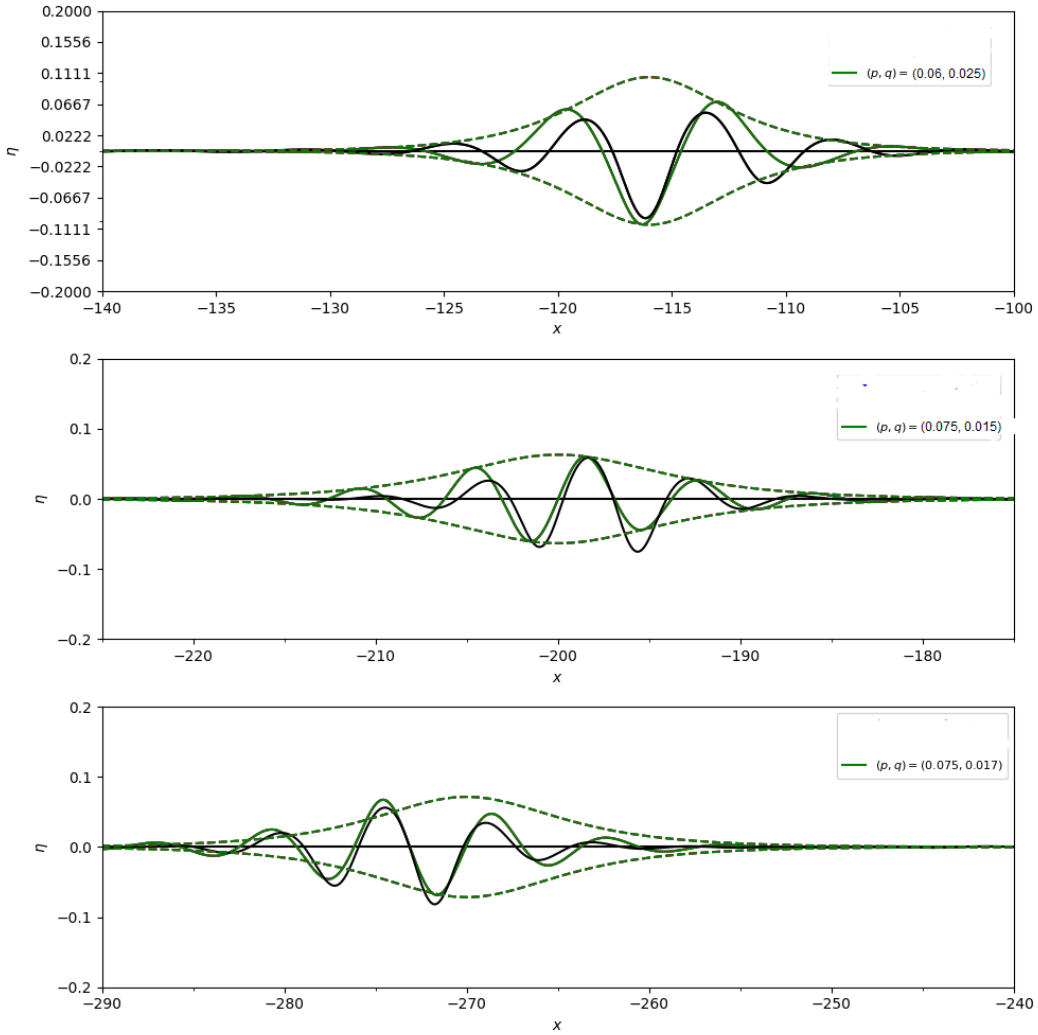

Figure 8: This figure shows 3 different breather solutions (black solid lines) overlayed with a wave envelope (green dotted line) and an analytical breather solution to the mKdV equation (green solid lines).

5 Concluding Remarks

The initial objective of finding the regions in parameter space under which breathers and wave-trains occur has almost been completed for background currents of 0.3 and 0.29. More simulations are needed to fill in the gaps of figures 6 and 7.

The phase speed of wave trains from the simulation and theoretical predictions were found to be agreement with minor discrepancies explained by non-linear effects which cause the simulation phase speeds to be larger than the theoretical results. The analytical breather solutions to the mKdV equation were also found to be a good fit to the simulation breathers.

As a next step, the propagation speeds of the analytical breather solutions using the (p, q) parameters can be computed and compared with the simulation speeds [3]. This will help

further determine whether the mKdV breather solutions are a suitable model for breathers in a stratified fluid.

To further comprehend the impact of background current on the occurrence of wave-trains and breathers, further simulations with background currents bigger than 0.3 and smaller than 0.29 are needed. In particular, background currents closer to the long-wave propagation speed $c_0 \approx 0.37$ may be of interest due to the possibility of a type of wave called "bores" being produced.

6 Acknowledgements

Special thanks must be given to my supervisor Dr. Kevin Lamb for their valuable mentorship and insights during this project.

References

[1] Acheson, D. J. (1992). *Elementary Fluid Dynamics.* , Clarendon Press.

[2] Drazin, P. G., Johnson, R. S. (1996). *Solitons: An introduction*. Cambridge Univ. Press.

[3] Nakayama, K., Lamb, K. G. (2020). Breathers in a three-layer fluid. *Journal of Fluid Mechanics*, 903. https://doi.org/10.1017/jfm.2020.653